



The effect of polycarboxylate shell of magnetite nanoparticles on protein corona formation in blood plasma



Márta Szekeres^{a,*}, Ildikó Y. Tóth^a, R. Turcu^b, Etelka Tombácz^a

^a Department of Physical Chemistry and Materials Sciences, University of Szeged, Hungary, 1 Aradi vt, 6720 Szeged, Hungary

^b National Institute R&D for Isotopic and Molecular Technology, Cluj-Napoca 400293, Romania

ARTICLE INFO

Keywords:

Magnetite nanoparticle
Protein corona
Polycarboxylate
Zeta potential
Colloidal stability

ABSTRACT

The development of protein corona around nanoparticles upon administration to the human body is responsible in a large part for their biodistribution, cell-internalization and toxicity or biocompatibility. We studied the influence of the chemical composition of polyelectrolyte shells (citric acid (CA) and poly(acrylic-co-maleic acid) (PAM)) of core-shell magnetite nanoparticles (MNPs) on the evolution of protein corona in human plasma (HP). The aggregation state and zeta potential of the particles were measured in the range of HP concentration between 1 and 80 (v/v)% 3 min and 20 h after dispersing the particles in HP diluted with Tris buffered saline. Naked MNPs aggregated in HP solution, but the carboxylated MNPs became stabilized colloiddally at higher plasma concentrations. Significant differences were observed at low plasma concentration. CA@MNPs aggregated instantly while the hydrodynamic diameter of PAM@MNP increased only slightly at 1–3 v/v % HP concentrations. The observed differences in protein corona formation can be explained by the differences in the steric effects of the polycarboxylate shells. It is interesting that relatively small but systematic changes in zeta potential alter the aggregation state significantly.

1. Introduction

Superparamagnetic iron oxide (SPIO) nanoparticles (designated here as MNP – short for magnetite nanoparticles) are effective agents for contrast enhancement in magnetic resonance imaging, magnetic drug delivery and release, and magnetic hyperthermia treatments [1–3]. MNPs with hydrodynamic diameters of 80–150 nm are cleared from the organism via the reticuloendothelial system (RES), while smaller particles can remain in the blood pool circulation for longer [4,5] providing the possibility for biomedical applications.

Proteins adsorb instantaneously on nanoparticle surfaces [6–8], which determines their fate in biological media by way of creating a bio-nano interface sensed by cells and other structures of the human body. A comprehensive review of our present knowledge on the interaction of proteins with nanoparticles and protein corona formation mechanisms in biorelevant media is given in the work of Rahman et al. [9]. The properties of protein coronas differ significantly depending on the surface chemistry of the nanoparticles and in turn, the surface chemistry has a deciding role not only in the formation of protein corona but also in the cellular uptake of the particles [6,10–12]. The main observations are that corona formation is largely affected by surface hydration or hydrophobicity, surface charge and the thickness

of the shell coating the nanoparticles. In some cases, even the absence of protein corona was detected on core-shell nanoparticles [10]. Systematic studies have been performed in order to test a wide range of polyelectrolytes (e.g., polyacrylic acid [10], polyethylene imine [13], polyethylene glycol [14,15], or natural polysaccharides [16]) to synthesize so called core-shell nanoparticles. Citric acid is also used frequently as surface modifier [e.g. 17, one of the most recent], albeit many studies reveal contraindications for in vivo application of citrate stabilized particles [18–20]. Modification of the chemistry of bio/nano interfaces allows for designing appropriate protein corona composition for specific biomedical aims. Proteomics studies are used efficiently for testing protein composition of coronas formed on various nanoparticles and the dynamics of corona formation [7,14,15]. Despite the vast amount of experimental data, further quantitative studies are needed to improve our insight into the mechanism and biomedical consequences of protein corona formation [21]. The effect of protein corona formation on colloidal stability of nanoparticles seems to be a neglected area.

Our aim was to study the effect of the composition of polycarboxylate coatings on the colloidal stability of magnetite nanoparticles (MNP) of ~8 nm in diameter [22,23] in buffered human plasma (HP) solutions at pH~7.4 in comparison to that of naked MNPs. The MNPs are coated by citrate (CA@MNP) and poly(acrylic-co-maleic acid)

* Corresponding author.

E-mail address: szekeres@chem.u-szeged.hu (M. Szekeres).

(PAM@MNP) according to previously published protocols [23,24]. Colloidal stability was tested in water at bio-relevant pH (~6.5) and the critical coagulation concentration (CCC) in NaCl solutions were found to be 1, 70 and 500 mM for MNP, CA@MNP and PAM@MNP, respectively [23,24]. Herein, we studied how much the in vitro formation of protein corona affects the aggregation propensity of these formulations. As biomedical application of citrate coated MNPs is frequently found in literature [e.g., 25], our aim was to test whether these particles can acquire sufficient colloidal stability in biological media due to protein corona formation. Human plasma was preferred versus human serum in our experiments (because the protein composition of the former is more similar to that of blood [26]) as well as versus whole blood (because the presence of micron-sized cells and platelets in whole blood would make DLS and zeta potential measurements impossible). The presence of coatings on MNP was verified with XPS measurements. The colloidal stability and zeta potential of the particles in HP solution media were studied in dynamic light scattering and electrokinetic measurements. The kinetics of protein corona formation and the effect of HP concentration on colloidal stability were also studied.

2. Materials and methods

Magnetite nanoparticles were synthesized using the method of coprecipitation of Fe(II) and Fe(III) salts as described in detail in [23]. The polyelectrolyte shells were formed around the MNP cores in the process of physico-chemical adsorption of citric acid (CA) monomers [24] and commercial PAM (Sigma-Aldrich) [24] polyelectrolyte. HCl, NaOH and NaCl (Molar, Hungary) were used to adjust the pH and ionic strength in the MNP, CA@MNP and PAM@MNP stock dispersions to pH ~6.5 and I=10 mM to ensure long term stability. The nanoparticle dispersions were then mixed with human plasma (HP) and Tris buffered saline (pH~7.4, I=0.154 M, Sigma-Aldrich) was used to adjust the volume to final HP concentrations. Ultrapure water (UP water, 18 M Ω) from a HumanCorp Zener water purification system was used in the experiments.

The chemical composition (atomic concentrations), as well as the chemical state of the atoms at the surface of CA- and PAM- coated MNPs (CA@MNP and PAM@MNP), were determined by X-ray Photoelectron Spectroscopy (XPS). The spectra were recorded using a spectrometer SPECS equipped with a dual-anode X-ray source Al/Mg, a PHOIBOS 150 2D CCD hemispherical energy analyzer and a multi-channeltron detector with vacuum maintained at 1×10^{-9} Torr. The Al $_{K\alpha}$ X-ray source (1486.6 eV) operated at 200 W was used for XPS investigations. The XPS survey spectra were recorded at 30 eV pass energy and 0.5 eV/step. The high-resolution spectra for individual elements were recorded by accumulating 10 scans at 30 eV pass energy and 0.1 eV/step. The powder suspensions were dried on an indium foil to allow the XPS measurements. The surface of the particles was cleaned by argon ion bombardment (300 V). Data analysis and curve fitting was performed using CasaXPS software with a Gaussian-Lorentzian product function and a non-linear Shirley background subtraction.

The blood of six healthy Donors (age of 30–64, five females and one male) was collected in the Institute of Laboratory Medicine of the University of Szeged according to the routine blood drawing practice of the Institute. Human plasma was separated from the blood in EDTA-anticoagulated tubes (Seditainer 1.8 vacutainer tubes, BD Inc., USA), using five tubes for each Donor, and then centrifuged. The plasma from all samples was pooled and a second step of centrifugation at 16,000 RPM for 10 min was applied to remove residual cells and cell debris. The total protein content was measured in the pooled sample as 65g/L. The within-subject and between-subject biological variation in total protein content is 2.75 and 4.7, respectively, based on Westgard database [27]. A plasma pool was used to get identical protein content in all experiments. After freeze drying the product in a Flexi-Dry μ P

lyophilizer (FTS Systems) using liquid nitrogen, it was stored at -18 °C in small aliquots and separately thawed at room temperature for individual experiments. For protein corona formation in HP, the thawed aliquots were dissolved in UP water to make up the original 100% concentration and Tris buffered saline solution (pH~7.4 and I~154 mM, Sigma-Aldrich) was used to dilute it to 1–80 v/v % for the experiments. The experiments with the bare and core-shell MNPs were performed in three replicates using separate plasma aliquots. Freeze dried rather than fresh plasma was adequate for the series of our room temperature experiments, as fresh plasma can only be stored for a maximum of three days while refrigerated.

The evolution of the average particle size of the PE@MNPs (i.e., magnetite nanoparticles with polyelectrolyte (PE) shells from CA and PAM) in the course of the protein corona formation was studied at 25 ± 0.1 °C both as a function of HP concentration and time (i.e., measured at 3 min and 20 h after MNP incubation in plasma). For particle size determination a Nano ZS (Malvern) dynamic light scattering apparatus was used applying a 4 mW He–Ne laser source ($\lambda=633$ nm) and operating in backscattering mode (at an angle of 173°). The pH and ionic strength was fixed at pH~7.4 and I~150 mM by the Tris buffered saline medium of HP solutions. The concentration of PE@MNPs was 0.1 g/l optimized in preliminary experiments. The aggregation state of the nanoparticles in the aqueous dispersions was characterized by the Z-average hydrodynamic diameter (Zave) values. We used the second- or third-order cumulant fit of the autocorrelation functions, depending on the degree of polydispersity. The variation of Zave values was less than 5% for primary particles but the error definition becomes irrelevant for large polydisperse aggregates.

The changes in the zeta potential due to protein corona formation were determined in electrophoretic mobility measurements at 25 ± 0.1 °C by using a Nano ZS (Malvern) apparatus with disposable zeta cells (DTS 1061). The experiments were performed at 20 h after MNP incubation in plasma. The zeta potentials were calculated with the help of the Smoluchowski equation. The accuracy of the measurements is ± 5 mV and the zeta-standard of Malvern (-55 ± 5 mV) was used for calibration. The dispersions were diluted to achieve an optimal intensity of ~105 counts per second and an ionic strength value of ~10 mM. Prior to the measurements, the samples were homogenized in an ultrasonic bath for 10 s, after which 2 min relaxation was allowed.

3. Results and discussion

Fig. 1 shows the C 1s spectra of the core-shell MNPs and the identification of peaks is seen in the figure caption. The XPS spectra clearly show the absence or presence of all chemical states of carbon characteristic of the coatings. Alcoholic groups (–C–OH) were found in the case of CA, while carboxylic groups (–C(O)–O) were found both in CA- and PAM-coated MNPs, which corresponds with the chemical structure of the coatings. Earlier FTIR-ATR experiments [23,24] revealed that both CA and PAM are bound to the MNPs via formation of inner-sphere Fe-carboxylate surface complexes the probable schemes of which are demonstrated in Fig. 1.

We chose room temperature for testing the effect of protein corona formation on hydrodynamic size, zeta potential and colloidal stability of the MNPs in human plasma. This is a frequent choice in literature [28,29] and, while inaccurate to mimic in vivo conditions [9], it is useful for comparing the in vitro behavior of different nanoparticles. For example, Mahmoudi et al. [30] found only a small deviation ($\sim \pm 1$ nm) between the hydrodynamic diameters of negatively charged polymer coated FePt nanoparticles ($r_{H\sim 5}$ nm) incubated in human serum albumin solutions in a 5 orders of magnitude concentration range when measured at temperatures of 13, 23 and 43 °C.

The hydrodynamic diameter of all MNPs (Fig. 2) increased at low plasma concentrations. The size increase is in the range of an order of magnitude for the naked and CA-coated MNPs, which is likely due to particle aggregation. PAM-coated particles were somewhat aggregated,

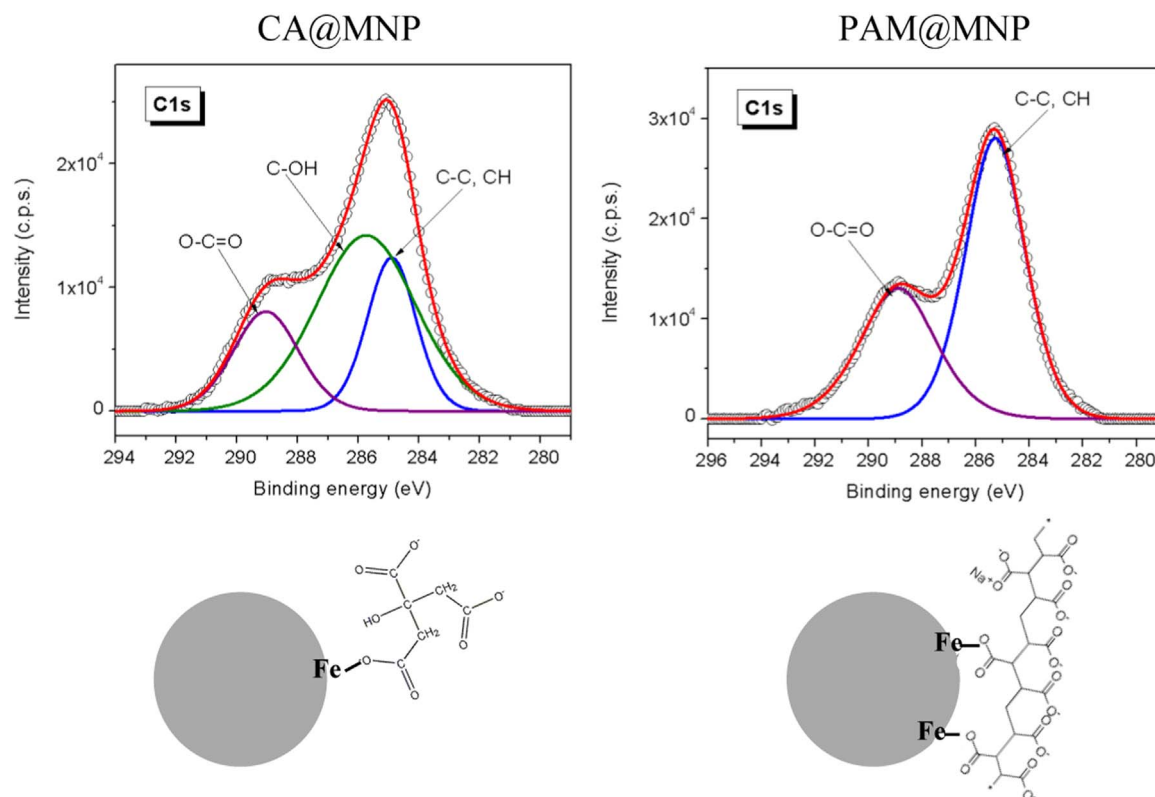


Fig. 1. C 1 s spectra of the core-shell MNPs and the schemes of Fe–O–C(O)–R binding between MNP iron sites and organic carboxylates. Peak positions for CA and PAM coated MNPs: C–C, CH 284.91 and 285.27 eV; O–C=O 289.05 and 288.9 eV, respectively, and C–OH 285.75 eV for CA@MNP.

but the size only doubled. With increasing HP concentration, the aggregates prevalent at lower HP concentrations cannot form because of the protecting effect of further HP protein adsorption and corona formation. Naked MNPs, however, remained aggregated in plasma – the smallest observed hydrodynamic size at the highest HP concentrations was ~400 nm. The size of the aggregates of the colloiddally

unstable dispersions of naked and CA-coated MNPs (at HP concentrations below 60 v/v % and between 1% and 10%, respectively) increased significantly with time (Fig. 2.b) revealing the absence of a full protein corona. The aggregation state of the dispersions was visualized in sedimentation experiments as demonstrated in Fig. 2.c. Visible sedimentation in the test tubes reveals the presence of aggregates. In the

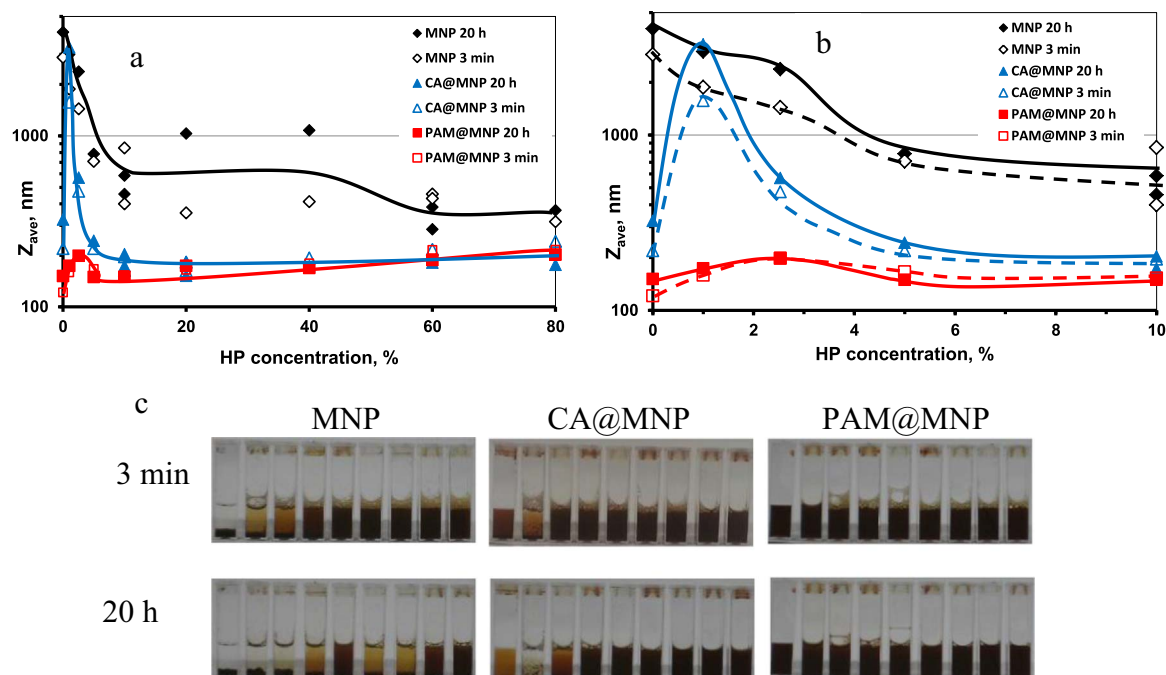


Fig. 2. Changes in the hydrodynamic diameter of naked MNP (black) and polyelectrolyte-coated MNPs CA@MNP, blue, and PAM@MNP, red in function of the concentration of HP measured 3 min and 20 h after dispersing them in HP solutions: panel (b) is the magnification of the plot in panel (a) in the low HP concentration range. In pictures (c) dispersions of MNP, CA@MNP and PAM@MNP in HP solutions of 0–80% concentration can be seen as taken at 3 min and 20 h after dispersion preparation.

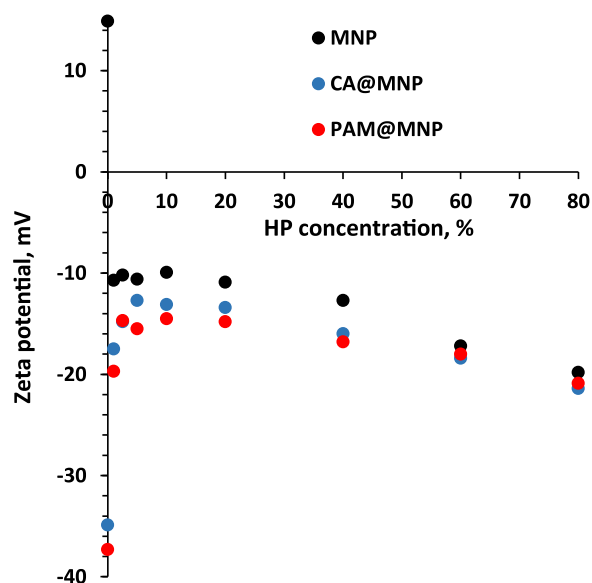


Fig. 3. Changes in the electrokinetic potential values of naked and core-shell MNPs in the course of protein corona formation in HP solutions prepared with Tris buffered saline solution as measured at 20 h after the MNP-HP dispersion preparation.

absence of plasma proteins, naked MNP is fully destabilized in Tris buffered saline (pH=7.4 and I=154 mM), while CA and PAM coating improved the stability. In cases when there is no visible sedimentation, both single particles and particle clusters with loose structure can be evenly distributed in the medium, which is the case at higher plasma concentrations for CA@MNP and at practically all plasma concentrations for PAM@MNP. Thus, we can hypothesize that abrupt changes in the hydrodynamic diameter of CA@MNP and PAM@MNP with plasma concentration are more likely due to nanoparticle aggregation/clustering, while the gradual and moderate increase can more likely be caused by the gradual increase in the thickness of the protein corona. Yallapu et al. [31] found somewhat different behavior of polyethylene glycol coated MNPs in human serum. Their particles in principle were uncharged and the serum lacks clothing factors, which can explain the absence of MNP aggregation in their experiments at low serum concentrations (i.e., no abrupt size increase was observed). However, they also observed the gradual increase in the hydrodynamic diameter from ~100 to 150–200 nm with increasing serum concentration, similar to our findings. Gradual increase in the nanoparticle size with plasma concentration was found by Monopoli et al. [32] for sulfonated polystyrene and silica nanoparticles. Vogt et al. [33] found a three-fold increase in the hydrodynamic diameter of silica-coated MNPs incubated in whole plasma, while the DLS size of dextrane-coated MNPs increased approximately by 30–40%. The general absence of observation of NP aggregation in literature can be due to the fact that the smallest plasma concentrations are above 5–10%, while we found strong aggregation at 1% and 2.53%. However, the comparison between literature data is not fully straightforward because, in general, the conditions of DLS measurements vary widely [34].

Notable changes in the hydrodynamic size were observed only under the conditions of probable aggregation, i.e., the average size of the aggregates increased with time. In contrast, the hydrodynamic size of PAM@MNPs in the whole HP concentration range and that of MNP and CA@MNP in HP of concentration higher than ~10 v/v % did not change practically with time showing the likely absence of aggregation.

The zeta potential changes in the course of protein corona formation (Fig. 3) showed a quite unusual picture. The decrease in originally negative values of zeta potential due to protein corona formation is fully consistent with literature and similar to that in many different studies [32]. On first encounter of HP proteins, naked and polyelectrolyte-coated MNPs (the original zeta potential of which is ~+15 and

~-35 mV, respectively) obtained negative potential values of similar magnitude (between ~-10 and ~-25 mV). Overcharging of the positively charged naked MNPs is in line with expectations, but the ~-15 mV charge compensation (from +15 to 0 mV) and the ~-10 mV overcharging (from 0 to -10 mV) would suggest the presence of an excess negative charge of adsorbed proteins in the order of -25 mV, which is five times of that of HP in solution (-5 mV). The ~10 mV decrease in the absolute values of negative zeta potentials of the core-shell MNPs to -25 mV is also against intuition. Further detailed electrokinetic potential studies are necessary to find the explanation of our first results, but it is clear that other specific interactions dominate over the general effects expected from physico-chemical charge-potential correlations.

After reaching an equilibrium state of the zeta potential of protein corona-coated MNPs at 10% concentration of HP medium, the negative values of zeta potentials begin to increase gradually with increasing plasma concentration. The latter observation is readily explained by the gradual adsorption of HP proteins introducing additional excess negative charges to the corona. Zeta potential measurements of protein corona coated nanoparticles in function of the protein source concentration were not found in our literature search range.

4. Conclusions

We studied the changes in hydrodynamic diameter and zeta potential of MNPs in the course of protein corona formation both as a function of human plasma concentration and time. The main findings follow from our studies as listed below.

- (i) Naked and CA-coated MNPs cannot be properly stabilized in human plasma due to protein corona formation. Allowing sufficient time for corona formation also does not lead to the formation of colloiddally stable dispersions.
- (ii) PAM coating stabilizes the MNPs efficiently at higher HP concentrations and the stability is practically independent of the time allowed for corona formation.
- (iii) Zeta potential measurements reveal the complex nature of the protein corona expressed as the complete absence of correlation between its nominal charge and zeta potential as it should be expected on the basis of general physical chemistry.
- (iv) Additionally, there is no correlation as well between the zeta potentials of the particles (with or without fully developed protein corona at higher or lower HP concentrations, respectively) and their observed colloiddal stability.

The latter two findings clearly show that further studies should be designed to clarify the mechanism of charge compensation in the course of protein corona formation around magnetite nanoparticles in human plasma.

Most importantly, we found that some MNP coatings, such as citric acid shell, for example, cannot protect the nanoparticles against aggregation if administered intravenously. Aggregated at the locus of IV injection, CA@MNPs should be able to redisperse in the blood stream in order to avoid blocking small arteries. Also further studies should clarify whether their redispersion in vivo is possible.

Acknowledgment

This research was supported by the OTKA (NK 84014) grant. Authors are thankful to Katalin Farkas and Imre Földesi (Institute of Laboratory Medicine, University of Szeged) for collecting and quantifying human plasma.

References

- [1] A.H. Latham, M.E. Williams, Controlling transport and chemical functionality of

- magnetic nanoparticles, *Acc. Chem. Res.* 41 (2008) 411–420.
- [2] S. Laurent, D. Forge, M. Port, A. Roch, C. Robic, L. Vander Elst, R.N. Muller, Magnetic iron oxide nanoparticles: synthesis, stabilization, vectorization, physico-chemical characterizations, and biological applications, *Chem. Rev.* 108 (2008) 2064–2110.
- [3] Y.-X.J. Wang, S. Xuan, M. Port, J.-M. Idee, Recent Advances in Superparamagnetic Iron Oxide Nanoparticles for Cellular Imaging and Targeted Therapy Research, *Curr. Pharm. Des.* 19 (2013) 6575–6593.
- [4] Y. Gossuin, P. Gillis, A. Hocq, Q.L. Vuong, A. Roch, Magnetic resonance relaxation properties of superparamagnetic particles, *Wiley Interdiscip. Rev. Nanomed. Nanobiotechnol.* 1 (2009) 299–310.
- [5] C. Corot, P. Robert, J.M. Idee, M. Port, Recent advances in iron oxide nanocrystal technology for medical imaging, *Adv. Drug Deliv. Rev.* 58 (2006) 1471–1504.
- [6] A. Lesniak, A. Campbell, M.P. Monopoli, I. Lynch, A. Salvati, K.A. Dawson, Serum heat inactivation affects protein corona composition and nanoparticle uptake, *Biomaterials* 31 (2010) 9511–9518.
- [7] A. Jedlovsky-Hajdu, F. Baldelli Bombelli, M.P. Monopoli, E. Tombácz, K.A. Dawson, Surface coatings shape the protein corona of spions with relevance to their application in vivo, *Langmuir* 28 (2012) 14983–14991.
- [8] P. Foroozandeh, A.A. Aziz, Merging worlds of nanomaterials and biological environment: factors governing protein corona formation on nanoparticles and its biological consequences, *Nanoscale Res. Lett.* 10 (2015) 221.
- [9] M. Rahman, S. Laurent, N. Tawil, L. Yahia, M. Mahmoudi, Protein-nanoparticle interactions, in: B. Martinac (Ed.) *Springer Series in Biophysics* 15, Springer-Verlag Berlin Heidelberg, 2013, pp. 21–44.
- [10] M. Safi, J. Courtois, M. Seigneuret, H. Conjeaud, J.-F. Berret, The effects of aggregation and protein corona on the cellular internalization of iron oxide nanoparticles, *Biomaterials* 32 (2011) 9353–9363.
- [11] M.A. Dobrovolskaia, B.W. Neun, S. Man, X. Ye, M. Hansen, A.K. Patri, R.M. Crist, S.E. McNeil, Protein corona composition does not accurately predict hematocompatibility of colloidal gold nanoparticles, *Nanomedicine* 10 (2014) 1453–1463.
- [12] Q. Peng, S. Zhang, Q. Yang, T. Zhang, X.Q. Wei, L. Jiang, C.-L. Zhang, Q.-M. Chen, Z.-R. Zhang, Y.-F. Lin, Preformed albumin corona, a protective coating for nanoparticles based drug delivery system, *Biomaterials* 34 (2013) 8521–8530.
- [13] M.P. Calatayud, B. Sanz, V. Raffa, C. Riggio, M.R. Ibarra, G.F. Goya, The effect of surface charge of functionalized Fe₃O₄ nanoparticles on protein adsorption and cell uptake, *Biomaterials* 35 (2014) 6389–6399.
- [14] S. Schöttler, G. Becker, S. Winzen, T. Steinbach, K. Mohr, K. Landfester, V. Mailänder, F.R. Wurm, Protein adsorption is required for stealth effect of poly(ethylene glycol)- and poly(phosphoester)-coated nanocarriers, *Nat. Nanotechnol.* 11 (2016) 372–377.
- [15] L. Landgraf, C. Christner, W. Storck, I. Schick, I. Krumborn, H. Dähring, K. Haedicke, K. Heinz-Herrmann, U. Teichgräber, J.R. Reichenbach, W. Tremel, S. Tenzer, I. Hilger, A plasma protein corona enhances the biocompatibility of Au@Fe₃O₄ Janus particles, *Biomaterials* 68 (2015) 77–88.
- [16] A. Lalatsa, E. Barbu, Carbohydrate nanoparticles for brain delivery, *Int. Rev. Neurobiol.* 130 (2016) 115–153.
- [17] C. Blanco-Andujar, D. Ortega, P. Southern, Q.A. Pankhurst, N.T. Thanh, High performance multi-core iron oxide nanoparticles for magnetic hyperthermia: microwave synthesis, and the role of core-to-core interactions, *Nanoscale* 7 (2015) 1768–1775.
- [18] S.J.H. Soenen, U. Himmelreich, N. Nuytten, T.R. Pisanic II, A. Ferrari, M. de Cuyper, Intracellular nanoparticle coating stability determines nanoparticle diagnostics efficacy and cell functionality, *Small* 6 (2010) 2136–2145.
- [19] S.J.H. Soenen, U.U. Himmelreich, E. Nuytten, M. de Cuyper, Cytotoxic effects of iron oxide nanoparticles and implications for safety in cell labelling, *Biomaterials* 32 (2011) 195–205.
- [20] V. Bastos, J.M. Ferreira de Oliveira, D. Brown, H. Jonhston, E. Malheiro, A.L. Daniel-da-Silva, I.F. Duarte, C. Santos, H. Oliveira, The influence of Citrate or PEG coating on silver nanoparticle toxicity to a human keratinocyte cell line, *Toxicol. Lett.* 249 (2016) 29–41.
- [21] P. del Pino, B. Pelaz, Q. Zhang, P. Maffre, G.U. Nienhaus, W.J. Parak, Protein corona formation around nanoparticles – from the past to the future, *Mater. Horiz.* 1 (2014) 301–313.
- [22] Z.-X. Sun, F.-W. Su, W. Forsling, P.-O. Samskog, Surface characteristics of magnetite in aqueous suspension, *J. Colloid Interface Sci.* 197 (1998) 151–159.
- [23] M. Szekeres, I.Y. Tóth, E. Illés, A. Hajdú, I. Zupkó, K. Farkas, G. Oszlánzi, L. Tiszlavicz, E. Tombácz, *Int. J. Mol. Sci.* 14 (2013) 14550–14574.
- [24] I.Y. Tóth, E. Illés, R.A. Bauer, D. Nesztor, M. Szekeres, I. Zupko, E. Tombácz, *Langmuir* 31 (2012) 16638–16646.
- [25] S. Wagner, J. Schnorr, A. Ludwig, V. Stang, M. Ebert, B. Hamm, M. Taupitz, Contrast-enhanced MR imaging of atherosclerosis using citrate-coated superparamagnetic iron oxide nanoparticles: calcifying microvesicles as imaging target for plaque characterization, *Int. J. Nanomed.* 8 (2013) 767–779.
- [26] V. Mirshafiee, R. Kim, M. Mahmoudi, M.L. Kraft, The importance of selecting a proper biological milieu for protein corona analysis in vitro: human plasma versus Human serum, *Int. J. Biochem. Cell Biol.* 75 (2016) 188–195.
- [27] Q. Westgard, *Desirable Biological Variation Database Specifications*, (<https://www.westgard.com/biodatabase1.htm>) (accessed 2016.10.19).
- [28] M. Schaffler, M. Semmler-Behnke, H. Sarioglu, S. Takenaka, A. Wenk, C. Schleh, S.M. Hauck, B.D. Johnston, W.G. Kreyling, Serum protein identification and quantification of the corona of 5, 15 and 80 nm gold nanoparticles, *Nanotechnology* 24 (2013) 265103.
- [29] M.A. Dobrovolskaia, A.K. Patri, J. Zheng, J.D. Clogston, N. Ayub, P. Aggarwal, B.W. Neun, J.B. Hall, S.E. McNeil, Interaction of colloidal gold nanoparticles with human blood: effects on particle size and analysis of plasma protein binding profiles, *Nanomedicine* 5 (2009) 106–117.
- [30] M. Mahmoudi, A.M. Abdelmonem, S. Behzadi, J.H. Clement, S. Dutz, M.R. Ejtehad, R. Hartmann, K. Kantner, U. Linne, P. Maffre, S. Metzler, M.K. Moghadam, C. Pfeiffer, M. Rezaei, P. Ruiz-Lozano, V. Serpooshan, M.A. Shokrgozar, G.U. Nienhaus, W.J. Parak, Temperature: the “Ignored” Factor at the NanoBio Interface, *ACS Nano* 7 (2013) 6555–6562.
- [31] M.M. Yallapu, N. Chauhan, S.F. Othman, V. Khalilzad-Sharghi, M.C. Ebeling, S. Khan, M. Jaggi, S.C. Chauhan, Implications of protein corona on physico-chemical and biological properties of magnetic nanoparticles, *Biomaterials* 46 (2015) 1–12.
- [32] M.P. Monopoli, D. Walczyk, A. Campbell, G. Elia, I. Lynch, F.B. Bombelli, K.A. Dawson, Physical-chemical aspects of protein corona: relevance to in vitro and in vivo biological impacts of nanoparticles, *J. Am. Chem. Soc.* 133 (2011) 2525–2534.
- [33] C. Vogt, M. Pernemalm, P. Kohonen, S. Laurent, K. Hultenby, M. Vahter, J. Lehtiö, M. S. Toprak, B. Fadeel Proteomics analysis reveals distinct corona composition on magnetic nanoparticles with different surface coatings: Implications for interactions with primary human macrophages, *PLOS ONE* (2015) (<http://journals.plos.org/plosone/article?id=10.1371/journal.pone.0129008>) (accessed 2016.10.19).
- [34] E. Brun, C. Sicard – Roselli, Could nanoparticle corona characterization help for biological consequence prediction?, *Cancer Nanotechnol.* 5 (2014) 7. <http://dx.doi.org/10.1186/s12645-014-0007-5>.